Journal of Photochemistry and Photobiology A: Chemistry 207 (2009) 274–281

Contents lists available at ScienceDirect

Journal of Photochemistry and Photobiology A: Chemistry

journal homepage: www.elsevier.com/locate/jphotochem

Analysis of photoinduced electron transfer in AppA

Nadtanet Nunthaboot[a], Fumio Tanaka[a,*], Sirirat Kokpol[b,c]

[a] Department of Chemistry, Faculty of Science, Mahasarakham University, SC-413, Mahasarakham 44150, Thailand
[b] Department of Chemistry, Faculty of Science, Chulalongkorn University, Bangkok 10330, Thailand
[c] Center of Excellence for Petroleum, Petrochemicals, and Advanced Materials, Chulalongkorn University, Bangkok 10330, Thailand

ARTICLE INFO

Article history:
Received 8 April 2009
Received in revised form 9 July 2009
Accepted 27 July 2009
Available online 3 August 2009

Keywords:
Photoreceptor
Photoinduced charge transfer
Molecular dynamic simulation
Semi-empirical molecular orbital method
BLUF
AppA
Analysis of fluorescence dynamics

ABSTRACT

The fluorescence dynamics of isoalloxazine (Iso) in AppA were analyzed in order to elucidate the mechanism of photoinduced electron transfer (ET) in a photosensing flavoprotein, blue-light sensing using flavin (BLUF) of AppA. The ET parameters contained in Kakitani and Mataga ET theory (KM theory) were determined by a non-linear least squares method using atomic coordinates obtained by molecular dynamic simulation (MD). The ET rate from Tyr21 to the excited state of isoalloxazine (Iso*) was slightly slower than that from Trp104 to Iso*. It was found that frequency factor ν_0 in the ET process from Tyr21 to Iso* was 16 times higher than the one from Tyr35 in a non-photosensing flavoprotein, flavin mononucleotide binding protein (FBP). Transferred charges and interaction energies in the systems of Iso*-Gln63-Trp104 and Iso*-Gln63-Tyr21 were obtained by a semi-empirical molecular orbital method (MO). Forty configurations of these systems by MD structures at 50 ps time intervals were geometrically optimized with the PM3 method. The mean charges at Iso* over 40 configurations were -0.254 ± 0.057 in the Iso*-Gln63-Trp104 system and 0.016 ± 0.002 in the Iso*-Gln63-Tyr21 system. Mean interaction energies among Iso*, Gln63 and Trp104 or Tyr21 were -11.7 ± 1.02 kcal/mol in the Iso*-Gln63-Trp104 system. The extraordinarily high ν_0 value in ET from Tyr21 to Iso* was elucidated by the H bond chain from Tyr21 to Iso* through Gln63, though MO results by PM3 could not elucidate it.

1. Introduction

Recently, a number of new flavoproteins have been found to function as photoreceptors. Among six families of the photoreceptors, phototropins [1], cryptochromes [2–5] and BLUF of AppA from *Rhodobacter sphaeroides* [6–15,17,18] contain flavins as the reaction centers. Recently BLUF from sources other than *R. sphaeroides* has been characterized [16,19–26]. In these flavin photoreceptors, cryptochromes and BLUF contain aromatic amino acids such as Trp and Tyr near Iso of flavins.

AppA functions as an anti-repressor of photosynthetic gene expression in the purple bacterium of *R. sphaeroides.* In vivo and in vitro analyses indicate that AppA contains two domains, a Cys-rich carboxy-terminal domain that is responsible for the isomerization of a disulfide bond in the photosynthetic repressor, PpsP, and an amino terminal domain that non-covalently binds with BLUF [6]. Full length AppA undergoes a photocycle with blue-light irradiation, causing a signaling state of flavin with a long-lived 10 nm red-shift of absorption spectrum [6]. Since BLUF of AppA does not function as a photosensor without Tyr21, Tyr21 is considered to play an essential role for it [7,8]. It was also demonstrated by FTIR that the hydrogen-bonding rearrangement between Iso and nearby amino acids takes place upon photo-excitation [10]. ET in WT and Y21F AppA [11,12] and in W104F AppA [13,14] was observed by means of fluorescence dynamics and transient absorption spectroscopy. In WT AppA, Iso* becomes Iso in the signaling state with lifetimes of 90 ps and 570 ps [11]. Strong evidence of ET in BLUF domain of Slr1694 was provided by ultrafast experiments [16], in which blue-light absorption was followed by the sequential formation of anionic $Iso^{-}\cdot$ and neutral IsoH· on a picosecond time scale. These results suggest that the formation of the signaling state is initiated by ET from Tyr21 and is followed by proton transfer. Structure of the signaling state of AppA was determined by an X-ray diffraction method [17]. Photophysics of AppA in the signaling state were also investigated by means of a transient absorption spectroscopy [18]. Regarding light absorption by AppA in the signaling state, Iso* decayed mono-exponentially with 7 ps lifetime to form the neutral IsoH·, which subsequently decayed to original Iso in the ground state within 60 ps.

Remarkable fluorescence quenching of Iso* has been also reported in many flavoenzymes other than photoreceptors [27–34]. In these flavoproteins, Trp and/or Tyr always exist near Iso. It was demonstrated by means of a picosecond-resolved [35,36] and femtosecond-resolved [37,38] transient absorption spectroscopy

* Corresponding author.
E-mail address: fukoh2003@yahoo.com (F. Tanaka).

1010-6030/$ – see front matter © 2009 Elsevier B.V. All rights reserved.
doi:10.1016/j.jphotochem.2009.07.020

that ET from Trp and/or Tyr to Iso* is responsible for the remarkable quenching. Ultrafast fluorescence dynamics of various flavoproteins have been investigated by an up-conversion technique [27–34]. Donor-acceptor distance-dependent ET rates in these flavoproteins have been expressed with center-to-center distance rather than edge-to-edge distance [31]. The distance-dependence of ET rates was analyzed with three kinds of ET theory [32].

FBP is considered to play an important role in electron transport process in the bacterium, but the whole picture of the electron flow and coupling of the redox proteins is not yet clear [39]. Three-dimensional structures of FBP from *Desulfovibrio vulgaris* (Miyazaki F) were determined by X-ray crystallography [40] and NMR spectroscopy [41]. According to these structures, Trp32 was closest to Iso and then Tyr35 and Trp106.

Various ET theories have been modeled for ET processes in bulk solution [42–50]. ET rate of FBP was much slower in crystal than in solution [33]. The ultrafast fluorescence dynamics of WT, W32Y and W32A FBP have been measured by means of the up-conversion method and compared among them [34]. The fluorescence decay of wild type (WT) FBP [51] was analyzed using MD coordinates and ET theories by Marcus [42–44], by Bixon and Jortner [45–47] and by KM theory [48–51]. In the analysis, electrostatic interaction energies between the Iso anion and other ionic groups, between Trp cations and other ionic groups, and between Tyr cation and other ionic groups, were introduced into ET theories. This greatly improved the agreement of calculated fluorescence decay with the observed one [51]. The fluorescence decays of WT, W32Y (Trp32 is replaced by Tyr32) and W32A (Trp32 is replaced by Ala32) FBP were also simultaneously analyzed to determine ET parameters contained in KM theory [52], where ET parameters for Trp and Tyr were separately determined. It was found that a frequency factor in KM theory was much higher in the ET process from Trp to Iso* than one from Tyr to Iso* [51–53].

ET process in AppA is very important because it is the initial step of the photocycle. It is not clear yet, however, whether ET takes place from Trp104 or from Tyr21. In the present work, we have analyzed fluorescence decay of WT AppA reported by Gauden et al. [11] with atomic coordinates in Iso, Trp104 and Tyr21 obtained by MD, and with KM theory. ET parameters obtained in AppA were compared to those in a non-photosensing flavoprotein of FBP. Amount of transferred charge and interaction energy both in Iso*-Gln63-Trp104 and Iso*-Gln-Tyr21 systems have studied by means of a semi-empirical MO.

2. Method of analyses

2.1. MD calculation

The initial structure of WT AppA was taken from X-ray structure [pdb code 1YRX] [9]. All missing hydrogen atoms of the protein were added using the LeaP module of the AMBER software package [54]. The parm99 force field [55] was used to describe the protein while force field parameters for the Iso were obtained from Schneider and Suhnel [56]. The AppA was solvated by 6494 TIP3P water molecules, respectively. To release bad contacts and to relax the system, the added water molecules were minimized, followed by energy minimization of the entire system. Afterwards, the whole system was heated from 10 K to 298 K over 50 ps and was further equilibrated under periodic boundary conditions at 298 K. The simulations were performed over 3000 ps. Data was collected during the 2000 ps (1000–3000 ps).

All MD calculations were carried out using the AMBER8 software package [54]. The system was set up under the isobaric-isothermal ensemble (NPT) with a constant pressure of 1 atm and constant temperature of 298 K. Electrostatic interaction was corrected by the Particle Mesh Ewald method [57]. The SHAKE algorithm [58] was employed to constrain all bonds involving hydrogen atoms. A cutoff distance of 1 nm was employed for a non-bonded pair interaction. MD calculations were performed with the time steps of 2 fs and coordinates of MD snapshot was collected every 0.01 ps.

2.2. ET theory

ET rate by KM theory [48–50] is expressed by Eq. (1):

$$k_{ET} = \frac{\nu_0}{1+\exp\{\beta(R-R_0)\}}\sqrt{\frac{k_BT}{4\pi\lambda_S}}\exp \times\left[-\frac{\{\Delta G^0 - e^2/\varepsilon_0 R + \lambda_S + ES\}^2}{4\lambda_S k_B T}\right] \quad (1)$$

Here ν_0 is an adiabatic frequency factor, β a coefficient related to ET process. R and R_0 are donor–acceptor distance and a critical donor–acceptor distance for ET process, respectively. R was expressed as a center-to-center distance rather than edge-to-edge distance [31,32,51,52]. ET process is adiabatic when $R < R_0$, and non-adiabatic when $R > R_0$. k_B, T and e are Boltzmann constant, temperature and electron charge, respectively. In the present work, we introduced an electrostatic energy, ES, in the proteins into KM theory, which is described later. λ_s is known as solvent reorganization energy [42] and expressed as Eq. (2):

$$\lambda_s = e^2\left(\frac{1}{2a_1}+\frac{1}{2a_2}-\frac{1}{R}\right)\left(\frac{1}{\varepsilon_\infty}-\frac{1}{\varepsilon_0}\right) \quad (2)$$

where a_1 and a_2 are radii of acceptor and donor when these reactants are assumed to be spherical, and ε_∞ and ε_0 are optical and static dielectric constants. The optical dielectric constant used was 2.0. The radii of Iso, Trp and Tyr were determined by the method described elsewhere [31,32,51,52]. The value of a_1 of Iso was 0.224 nm, and a_2 for Trp and Tyr was 0.196 nm and 0.173 nm, respectively.

The standard free energy change was expressed with ionization potential of ET donor, E_{IP}, as Eq. (3):

$$\Delta G^0 = E_{IP} - G^0_{Iso} \quad (3)$$

G^0_{Iso} is standard Gibbs energy related to electron affinity of Iso*. E_{IP}'s of Trp and Tyr used for the analysis were 7.2 eV and 8.0 eV, respectively [59].

2.3. Electrostatic energy in the protein

Protein systems contain many ionic groups, which may influence ET rate. *ES* between Iso^- and all ionic amino acid residues including phosphate anions of FMN (*ES*(*Iso*)), between $Trp104^+$ and all ionic amino acid residues including phosphate anions of FMN (*ES*(*Trp*104)), as well as between $Tyr21^+$ and all ionic amino acid residues including phosphate anions of FMN (*ES*(*Tyr*21)) are expressed by Eqs. (4)–(6), respectively. AppA contains 8 Glu's, 1 Asp, 5 Lys's, 11 Arg's and 2 negative charges at FMN phosphate.

$$ES(Iso) = \sum_{i=1}^{8}\frac{C_{Iso}\cdot C_{Glu}}{\varepsilon_0 R_{Iso}(Glu\text{-}i)} + \sum_{i=1}^{1}\frac{C_{Iso}\cdot C_{Asp}}{\varepsilon_0 R_{Iso}(Asp\text{-}i)} + \sum_{i=1}^{5}\frac{C_{Iso}\cdot C_{Lys}}{\varepsilon_0 R_{Iso}(Lys\text{-}i)} + \sum_{i=1}^{11}\frac{C_{Iso}\cdot C_{Arg}}{\varepsilon_0 R_{Iso}(Arg\text{-}i)} + \sum_{i=1}^{2}\frac{C_{Iso}\cdot C_{P}}{\varepsilon_0 R_{Iso}(P\text{-}i)} \quad (4)$$

$$ES(Trp104) = \sum_{i=1}^{8} \frac{C_{104} \cdot C_{Glu}}{\varepsilon_0 R_{104}(Glu\text{-}i)} + \sum_{i=1}^{1} \frac{C_{104} \cdot C_{Asp}}{\varepsilon_0 R_{104}(Asp\text{-}i)} + \sum_{i=1}^{5} \frac{C_{104} \cdot C_{Lys}}{\varepsilon_0 R_{104}(Lys\text{-}i)} + \sum_{i=1}^{11} \frac{C_{104} \cdot C_{Arg}}{\varepsilon_0 R_{104}(Arg\text{-}i)} + \sum_{i=1}^{2} \frac{C_{104} \cdot C_P}{\varepsilon_0 R_{104}(P\text{-}i)} \quad (5)$$

$$ES(Tyr21) = \sum_{i=1}^{8} \frac{C_{21} \cdot C_{Glu}}{\varepsilon_0 R_{21}(Glu\text{-}i)} + \sum_{i=1}^{1} \frac{C_{21} \cdot C_{Asp}}{\varepsilon_0 R_{21}(Asp\text{-}i)} + \sum_{i=1}^{5} \frac{C_{21} \cdot C_{Lys}}{\varepsilon_0 R_{21}(Lys\text{-}i)} + \sum_{i=1}^{11} \frac{C_{21} \cdot C_{Arg}}{\varepsilon_0 R_{21}(Arg\text{-}i)} + \sum_{i=1}^{2} \frac{C_{21} \cdot C_P}{\varepsilon_0 R_{21}(P\text{-}i)} \quad (6)$$

In Eqs. (4)–(6), C_{Iso} is the charge of Iso anion and is equal to $-e$. C_{104} and C_{21} are the charges of Trp104 cation and Tyr21 cation, respectively, and both equal to $+e$. C_{Glu} and C_{Asp} are the charges of Glu and Asp in AppA, respectively, and equal to $-e$. C_{Lys} and C_{Arg} are the charges of Lys and Arg, respectively, and equal to $+e$. C_P is the charge of phosphate of FMN and equal to $-e$. We assumed that these groups are all in an ionic state in solution. Distances between Iso and ith Glu (i = 1–8) are denoted as $R_{Iso}(Glu\text{-}i)$. Distances between Trp104 and ith Glu (i = 1–8) are denoted as $R_{104}(Glu\text{-}i)$, and so on.

ES in Eq. (1) was expressed as follows:

$$\text{For } k_{ET}^{Trp}(t'), \quad ES = ES(Iso) + ES(Trp104) \quad (7)$$

$$\text{For } k_{ET}^{Tyr}(t'), \quad ES = ES(Iso) + ES(Tyr21) \quad (8)$$

$k_{ET}^{Trp}(t')$ and $k_{ET}^{Tyr}(t')$ denote ET rates from Trp and Tyr to Iso*, respectively.

2.4. Observed and calculated fluorescence decays

Fluorescence decay function was reported by Gauden et al. [11], which is expressed by Eq. (9):

$$F_{obs}(t) = 0.10 \exp\left(\frac{-t}{25}\right) + 0.32 \exp\left(\frac{-t}{150}\right) + 0.56 \exp\left(\frac{-t}{670}\right) + 0.02 \exp\left(\frac{-t}{3800}\right) \quad (9)$$

The lifetimes were expressed in ps unit. The calculated decay [51,52,60] was expressed as Eq. (11).

$$F_{calc}(t) = \left\langle \exp - \{k_{ET}^{Trp104}(t') + k_{ET}^{Tyr21}(t')\}t \right\rangle_{AV} \quad (10)$$

$k_{ET}^{Trp104}(t')$ and $k_{ET}^{Tyr21}(t')$ are ET rates from Trp104 and from Tyr21 to Iso*, respectively, which are given by Eq. (1). $\langle \ldots \rangle_{AV}$ means averaging procedure of the exponential function in Eq. (10) over t' up to 2 ns at 0.1 ps time intervals. In Eq. (10), we assumed that the decay function during MD time range can be always expressed by an exponential function at any instant of time, t'. Comparison between our method and one given by Henry and Hochstrasser [60] was described in Supplemental Material.

2.5. Determination of ET parameters

Unknown ET parameters in Eq. (1) were ν_0 (Trp104), ν_0 (Tyr21), β (Trp104), β (Tyr21), R_0 (Trp104), R_0 (Tyr21), G_{Iso}^0 and ε_0. These parameters were determined so as to obtain the minimum value of χ^2 defined by Eq. (11), by means of a non-linear least squares method, according to Marquardt algorithm.

$$\chi^2 = \frac{1}{N} \sum_{i=1}^{N} \frac{\{F_{calc}(t_i) - F_{obs}(t_i)\}^2}{F_{calc}(t_i)} \quad (11)$$

N denotes number of time intervals (1 ps) and was 1300. Eq. (12) expresses deviations between the observed and calculated intensities.

$$\text{Deviation } (t_i) = \frac{F_{calc}(t_i) - F_{obs}(t_i)}{\sqrt{F_{calc}(t_i)}} \quad (12)$$

2.6. MO calculation

Atomic coordinates of Iso, Trp104, Tyr21 and Gln63 were obtained from MD data. Iso was substituted with lumiflavin, Trp104 with 3-methylindole, Tyr21 with 4-methylphenol and Gln63 with propanamide. Atomic coordinates of these compounds were obtained from 40 MD structures with 50 ps time intervals up to 2 ns. Molecular orbital calculations were performed with WinMOPAC software [Professional, Version 3.9; Fujitsu, Tokyo]. Geometries of Iso-Gln63-Trp104 and Iso-Gln63-Tyr21 systems were optimized with a semi-empirical MO of PM3. Key words used for MO calculations were EF, PM3, PRECISE, EXCITED, XYZ, GEO-OK and EPS (visit for meaning of these Keywords: http://openmopac.net/). The value of ε_0 (static dielectric constant) used was 29 obtained from the result of ET analyses as mean of ε_0 obtained by Method 1 (see Table 1). Interaction energy (ΔE) among Iso*, Gln and Trp or Tyr was evaluated by Eq. (13) [53]:

$$\Delta E = \Delta H_f(Iso^*\text{-}Gln\text{-}AA) - \{\Delta H_f(Iso^*) + \Delta H_f(Gln) + \Delta H_f(AA)\} \quad (13)$$

In Eq. (13), ΔIso*Gln-AA denotes a heat of formation in a system of Iso*-Gln-AA, where AA denotes Trp104 or Tyr21. $\Delta H_f(Iso^*)$, $\Delta H_f(Gln)$ and $\Delta H_f(AA)$ are heat of formation in the systems of only Iso*, of only Gln63, and of only AA in the ground state, respectively. The heat of formation contains total electronic energy, core–core repulsion energy between atoms and heat of formation of all constituent atoms.

Table 1
ET parameters in AppA.[a]

Method of analysis	ET parameters for Trp104			ET parameters for Tyr21			G_{Iso}^0 (eV)	ε_0	χ^{2b}
	ν_0 (ps^{-1})	β (nm^{-1})	R_0 (nm)	ν_0 (ps^{-1})	β (nm^{-1})	R_0 (nm)			
1[c]	2228	60.1	0.694	3226	6.25	2.72	8.82[d]	28.9	2.86×10^{-6}
2[c]	1016[e]	21.0[e]	0.557	197[e]	6.25[e]	0.678	8.66[f]	20.3	2.92×10^{-4}

[a] KM theory was used for the analyses [48–50]. [b] Chi square between the observed and calculated fluorescence intensities give by Eq. (11). [c] Fluorescence decay parameters were τ_1 = 25 ps (α_1 = 0.10), τ_2 = 150 ps (α_2 = 0.32), τ_3 = 670 ps (α_3 = 0.56), τ_4 = 3.8 ns (α_4 = 0.02) [11]. [d] $\Delta G_{Trp}^0 = -1.42$ eV and $\Delta G_{Tyr}^0 = -0.618$ eV. [e] ET parameters were obtained by Nunthaboot et al. [52], and fixed during best-fit procedure. [f] $\Delta G_{Trp}^0 = -1.82$ eV and $\Delta G_{Tyr}^0 = -0.82$ eV.

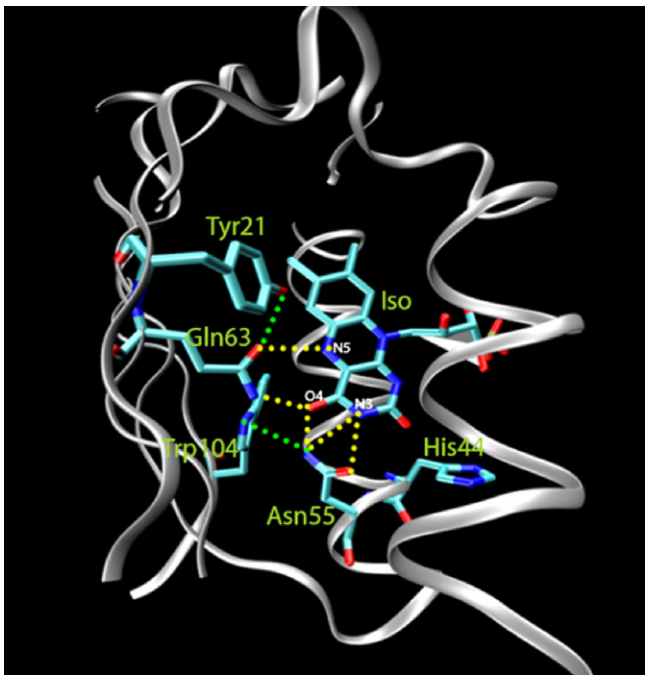

Fig. 1. A snapshot of MD structures of AppA. Potential H bond pairs (distances below 0.35 nm) are indicated with dotted lines. H bond interactions between amino acid-amino acid and between amino acid and Iso are shown with green and yellow colors, respectively. (For interpretation of the references to color in this figure legend, the reader is referred to the web version of the article." has been incorporated in the caption to Fig. 1. Please check.)

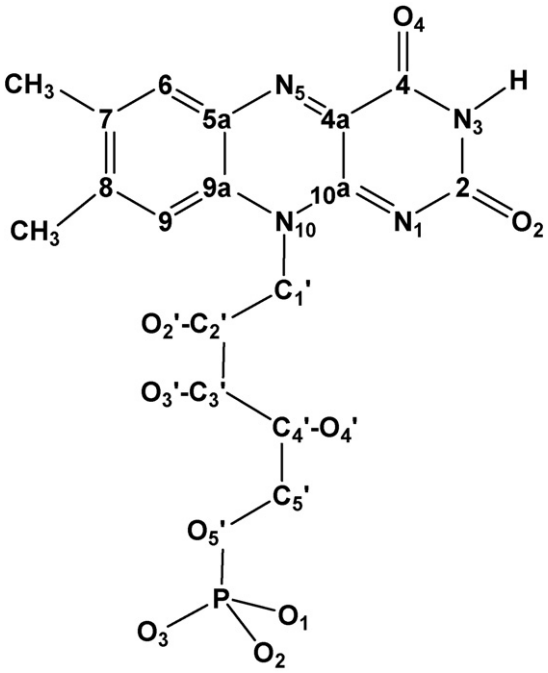

Fig. 2. Chemical structure and atom notations of FMN.

3. Results

3.1. MD geometries of AppA at Iso binding site

Fig. 1 shows a snapshot of MD configurations around the Iso binding site. Potential hydrogen-bonding (H bond) pairs were indicated by dotted lines. Dynamic properties of H bonds were described in the next section. Chemical structure and atom notations of flavin mononucleotide (FMN) are illustrated in Fig. 2. Time-dependent changes in the distances between Iso and Trp104 or Tyr21 are shown in Fig. 3. Mean center-to-center distances (*Rc*) over MD time range were 0.89 nm between Iso and Trp104, and 0.80 nm between Iso and Tyr21. Mean edge-to-edge distances (*Re*) were 0.32 nm between Iso and Trp104 and 0.28 nm between Iso and Tyr21. Both mean distances were a little shorter in Iso-Tyr21 system than in Iso-Trp104 system. Fig. 4 shows time-dependent changes in inter-planar angles between Iso and Trp104 or Tyr21. Mean angles were −60.1° between Iso and Trp104 and 72.2° between Iso and Tyr21.

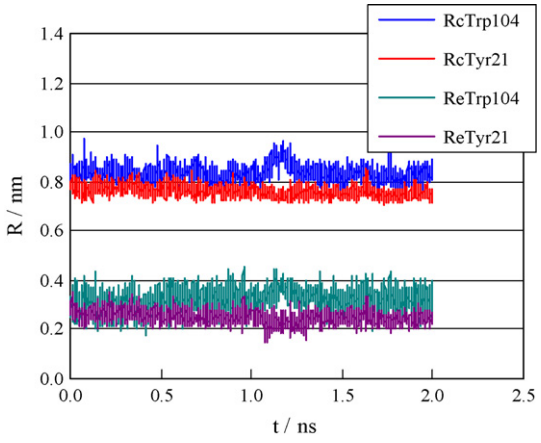

Fig. 3. Time-dependent change in the distances between Iso and Trp104 or Tyr21 in AppA. *Rc* and *Re* denote center-to-center distance and edge-to-edge distance, respectively.

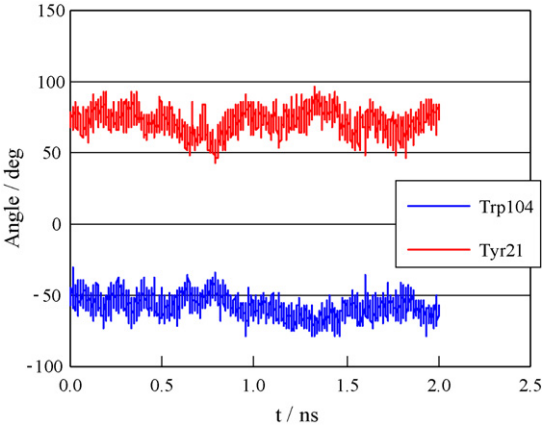

Fig. 4. Inter-planer angle between Iso and nearby aromatic amino acids. Trp104 and Tyr21 denote the angles between Iso and Trp104 and between Iso and Tyr21, respectively.

3.2. Time-dependent change in H bond formation

H bond formation is static in X-ray structure in general, but dynamic in solution as predicted by Obanayama et al. [61]. Fig. S1 shows distances between three atomic pairs of potential proton donor and acceptor, IsoO4/Gln63NH, IsoO4/Asn45NH, and IsoN3H/Asn45O. Fig. 5 demonstrates sudden changes in the distances among Trp104NH, Gln63O, Gln63N and Tyr21OH. Distances between TyrOH and GlnO are mostly within H bond distance. The distance, however, suddenly changed from 0.28 nm to 0.52 nm around 1.1 ns. This change in the distance well correlated with sudden changes in the other distances between Trp104NH and Gln63N, between Trp104NH and Gln63O, and between Tyr21OH and Gln63N. The sudden changes in the distances may be eluci-

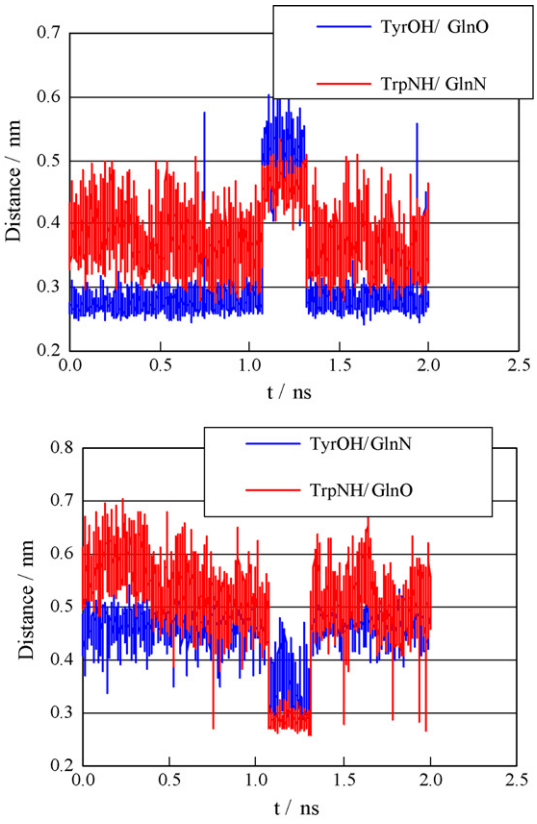

Fig. 5. Internal rotation of Gln63 and H bond switching. Inserts show H bond pairs. Tyr, Trp and Gln denote Tyr21, Trp104 and Gln63, respectively.

dated by internal rotation of Gln63 side chain. Though in H bond pairs of IsoO4/Gln63NH, IsoO4/Asn45NH, and IsoN3H/Asn45O the mean distances over MD time range were longer than H bond distance (0.28 nm), the distances were quite often within the H bond distance.

Fig. 6 shows distributions of inter-atomic distances between potential H bond pairs. The mean distances over MD time range were 0.36 nm in IsoN5/Gln63O, 0.31 nm in IsoO4/Gln63NH, 0.30 nm in IsoO4/Asn45NH, 0.30 nm in IsoN3/Asn45O, 0.35 nm

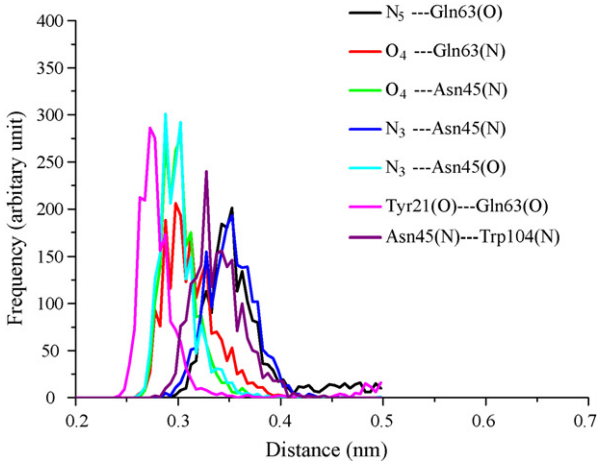

Fig. 6. Distribution of the distance between potential proton donor and acceptor near Iso. Insert indicates H bond pairs. The mean distances over MD time range were 0.36 nm in N5-Gln63O, 0.31 nm in O4-Gln63NH, 0.30 nm in O4-Asn45NH, 0.30 nm in N3-Asn45O, 0.35 nm in N3-Asn45NH, 0.38 nm in Trp104NH-Asn45NH, and 0.31 nm in Tyr21OH-Gln63O.

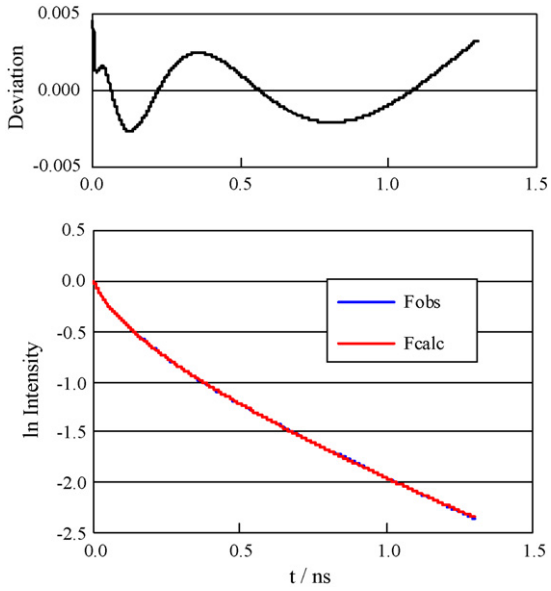

Fig. 7. Fluorescence decays of AppA. Fobs and Fcalc denote the observed and calculated fluorescence decay functions. Fobs were taken from Gauden et al. [11], of which decay parameters are listed at footnote of Table 1. Deviation denotes the difference between the observed and calculated fluorescence decays, as defined by Eq. (12). All of 8 ET parameters were determined independently by means of the non-linear least squares method as described in txt, and listed in Table 1 as Method 1. The value of χ^2 was 2.86×10^{-6}.

in IsoN3/Asn45NH, 0.38 nm in Trp104NH/Asn45NH, 0.31 nm in Tyr21OH/Gln63O. In O4/Gln63NH, O4/Asn45NH, and N3H/Asn45O atomic pairs, the maximum distributions of the distances were around 0.3 nm, but appreciable distributions of the distance were found within H bond distance. In the Tyr21OH/Gln63O pair minor maximum distribution was found around 0.52 nm due to the flip-flop rotation of Gln63 as stated above, in addition to the main maximum distribution around 0.28 nm. These results suggest that H bond of Tyr21OH/Gln63O is quite tight, and Gln63O may also form H bond with IsoN5. Gln63NH formed H bond with IsoO4.

3.3. Analysis of fluorescence decay

The observed fluorescence decay expressed by Eq. (9) was analyzed with KM theory and atomic coordinates obtained by MD. Fig. 7 shows the observed fluorescence decay by Gauden et al. [11] and the calculated decay with best-fit ET parameters (Method 1). Deviation between the decays defined by Eq. (12) is shown at the upper panel. Agreement between the two decays was excellent. The value of χ^2 was 2.86×10^{-6}. ET parameters obtained by the best-fit procedure are listed in Table 1. In the previous work [52], we have obtained ET parameters for Trp and Tyr common among WT, W32Y and W32A FBP. The decay by Gauden et al. [11] was analyzed using the values of ν_0 (Trp104), ν_0 (Tyr21), β (Trp104), and β (Tyr21) obtained in FBP [52]. Fluorescence decays obtained with these ET parameters are shown in Fig. S2 (Method 2). The value of χ^2 by Method 2 was 2.92×10^{-4}. The calculated decay by Method 1 reproduced the observed decay much better than one by Method 2. Results of these analyses are also listed in Table 1.

3.4. ET parameters

ET parameters in Eq. (1) obtained were ν_0 (Trp104) = 2228 ps^{-1} and ν_0 (Tyr21) = 3226 ps^{-1} by Method 1, while ν_0 (Trp) and ν_0 (Tyr) were 1016 ps^{-1} and 197 ps^{-1} by Method 2, respectively. The value of ν_0 (Trp) by Method 1 was about twice of one by Method 2, and the

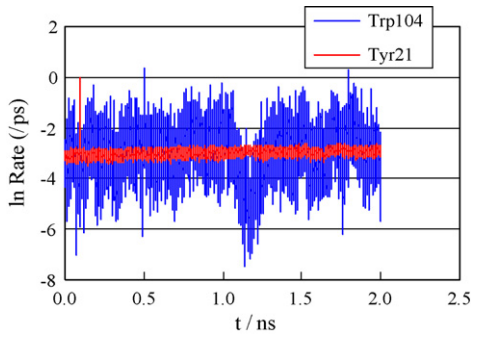

Fig. 8. Time-dependent ET rate from Trp104 and Tyr21 to Iso* obtained with Method 1. Trp104 and Tyr21 indicate ET rate from Trp104 and from Tyr21 to Iso*, respectively. ET rates were calculated with ET parameters listed in Table 1 as Method 1.

values of ν_0 (Tyr) by Method 1 was about 16 times of one by Method 2. The value of β (Trp104) by Method 1 was about 2.9 times of one by Method 2. The value of R_0 (Trp104) was quite similar between two Methods. The value of R_0 (Tyr21) by Method 1 was about 4 times of one by Method 2. The other ET parameters of G^0_{Iso} and ε_0 were quite similar between the two Methods. Most remarkable difference between AppA (Methods 1) and FBP (Method 2) was found in ν_0 (Tyr).

3.5. Time-dependent change in ET rate

Time-dependent changes in ET rate obtained by Method 1 are shown in Fig. 8. ET rate from Trp104 varied much with time, while one from Tyr21 was quite constant. Mean ET rates over MD time range from Trp104 to Iso* and from Tyr21 to Iso* obtained by Method 1 were 0.00118 ps^{-1} (lifetime 0.851 ns) and 0.00099 ps^{-1} (lifetime 1.01 ns), respectively. The result suggests that ET rate is a little faster from Trp104 to Iso* than from Tyr21 to Iso*. If we use ET parameter for ν_0 and β obtained by FBP (Method 2), ET rate from Trp104 to Iso* should be much faster than one from Tyr21 to Iso*, as shown in Fig. S3.

3.6. Electrostatic energy in AppA

Time-dependent changes in electrostatic energies obtained by Method 1 are shown in Fig. S4. Eiso, E104 and E21 in Fig. S4 denote the energies at Iso^-, $Trp104^+$ and $Tyr21^+$. Eiso was always positive, and E104 and E21 were always negative, which are quite different from FBP [52]. In WT FBP the electrostatic energies of all ET donors and acceptor were positive or around zero.

3.7. Photoinduced charge transfer and interaction energy between Iso* and ET donors

Molecular interactions among Iso*, Gln63 and Trp104 or Tyr21 were calculated with 40 MD structures with time intervals of 50 ps over 2 ns range. Physical quantities obtained by MO are listed in Table 2. Fig. 9 shows time-dependent changes in dipole moments of the Iso*-Gln63-Trp104 system and of the Iso*-Gln63-Tyr21 system. The dipole moment drastically varied with time from 10 D to 30 D in the Iso*-Gln63-Trp104 system. The dipole moment in the Iso*-Gln63-Tyr21 system, however, varied a little around 7–10 D and sometimes up to 18 D around 1.2 ns of MD time when H bond switching from Tyr21OH/Gln63O to Tyr21OH/Gln63NH took place due to internal rotation of Gln63 as shown in Fig. 5. Fig. 10 shows typical direction and magnitude of dipole moments in the Iso*-Gln63-Trp104 system and the Iso*-Gln63-Tyr21 system. In the Iso*-Gln63-Trp104 system, the direction was from Iso ring to

Table 2
Physical quantity obtained by PM3.[a]

Physical quantity	Iso*-Gln63-Trp104	Iso*-Gln63-Tyr21
Heat of formation (kcal/mol)	−22.7 ± 1.02	−73.4 ± 0.15
Charge		
Iso*	−0.254 ± 0.057	0.016 ± 0.002
AA[b]	0.257 ± 0.057	−0.025 ± 0.002
Gln63	0.003 ± 0.003	0.009 ± 0.003
Dipole moment (D)	13.9 ± 1.07	9.21 ± 0.50
Interaction energy (kcal/mol)[c]	−11.7 ± 1.02	1.28 ± 0.15

[a] Conformations of model molecules, Iso, Trp104, Tyr21 and Gln63 were constructed from 40 MD structures at time intervals of 50 ps over 2 ns. Lumiflavin as Iso, 3-methylindole as Trp104, 4-methylphenol as Tyr21 and propanamide as Gln63 were used for the PM3 calculations. The quantities ±SE were indicated.
[b] AA denotes aromatic amino acid as Trp104 or Tyr21.
[c] The interaction energy was obtained by Eq. (13) in text.

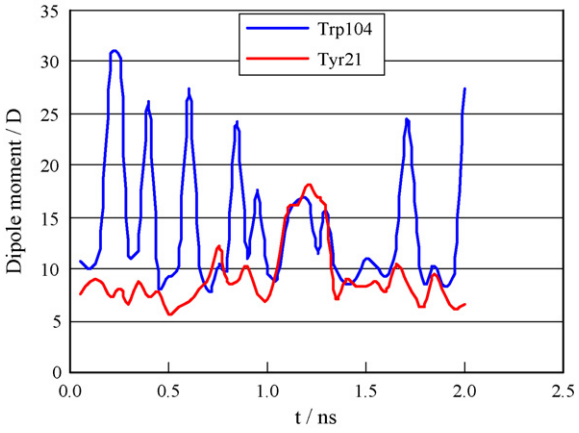

Fig. 9. Time-dependent change in dipole moments of Iso*-Gln63-Trp104 system and Iso*-Gln63-Tyr21 system. Trp104 and Tyr21 denote Iso*-Gln63-Trp104 system and Iso*-Gln63-Tyr21 system, respectively.

Trp104 ring and further, the magnitude of dipole moment was 30.5 D. This suggests that the electron transfers from Trp104 to Iso*. Contrary to this, in the Iso*-Gln63-Tyr21 system, the direction of dipole moment was almost in plane of Iso*. Since dipole

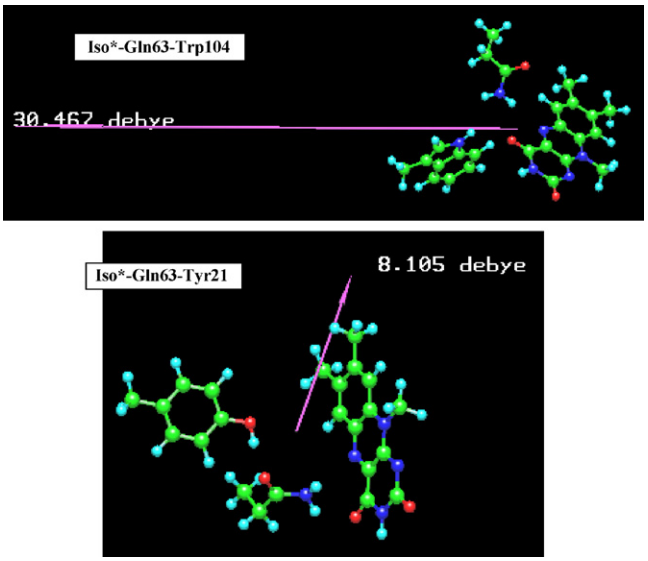

Fig. 10. Typical direction and magnitude of dipole moment. MO calculations were performed by PM3 method. Initial structures of Iso-Gln63-Trp104 and Iso-Gln63-Tyr21 systems were obtained from MD structures at 250 ps of MD time. Directions and magnitudes of dipole moments were indicated by arrows in the both systems.

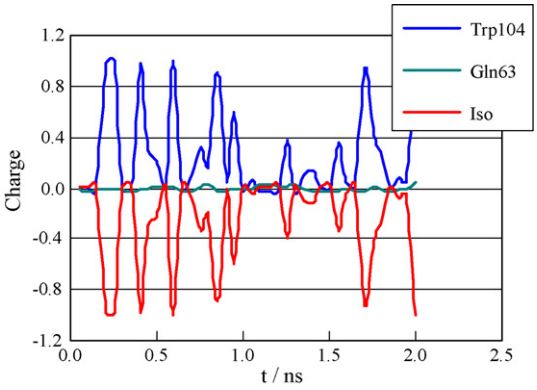

Fig. 11. Time-dependent change in charge in Iso*-Gln63-Trp106 system. Charge was obtained by summing up Mulliken charges at all atoms in Iso*, Gln63 and Trp104. Trp104, Gln63 and Iso indicate charge densities of these model molecules.

moment of Iso* alone is around 10 D with the direction in the plane of Iso*, ET in the Iso*-Gln63-Tyr21 system could not be explained by PM3 method. Fig. 11 shows time-dependent change in charge at Iso*, Gln63 and Trp104 in the Iso*-Gln63-Trp104 system. Amount of negative charge at Iso* seemed to correlate with positive charge at Trp104. In Iso*-Gln63-Tyr21 system the amount of charge was little at any model compounds. The H bond distances with geometrically optimized structures by PM3 are shown in Fig. S5. Frequencies of H bond formation between Tyr21OH and Gln63O, and between Gln63NH and Iso*O4 were quite high. This also supports H bond net from Tyr21 to Iso* through Gln63. Fig. 12 shows the interaction energies in the Iso*-Gln63-Trp104 system and in the Iso*-Gln63-Tyr21 system obtained by Eq. (13). In Iso*-Gln63-Trp104 system the interaction energy was almost always negative, while in Iso*-Gln63-Tyr21 system it was a little positive. In the Iso*-Gln63-Trp104 system, photoinduced charge transfer (CT) takes place from Trp104 to Iso* and so the interaction energy was negative.

3.8. Polarity around ET donors and acceptor

Static dielectric constant ε_0 (=29) in AppA was quite high compared to ε_0 (=9.9) in FBP [52]. Fig. 13 shows a radial distribution function of water molecules near FMN. The radial distribution function suggested that two water molecules present around Iso near O4 and N5 in AppA, while only one near O4 in FBP (manuscript in preparation). Ionic amino acid residues may also influence the

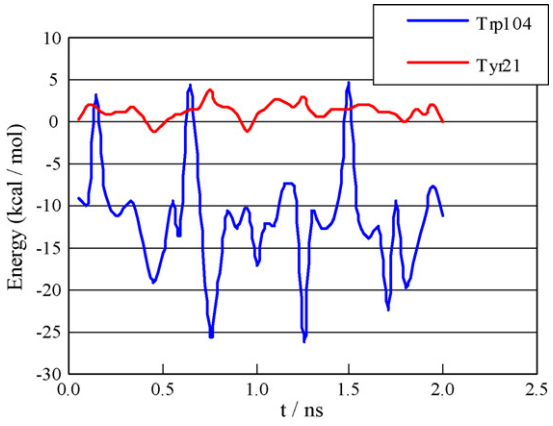

Fig. 12. Time-dependent change in the interaction energy among chromophores. Trp104 and Tyr21 indicate Iso*-Gln63-Trp104 system and Iso*-Gln63-Tyr21 system, respectively. The interaction energy was obtained by Eq. (13).

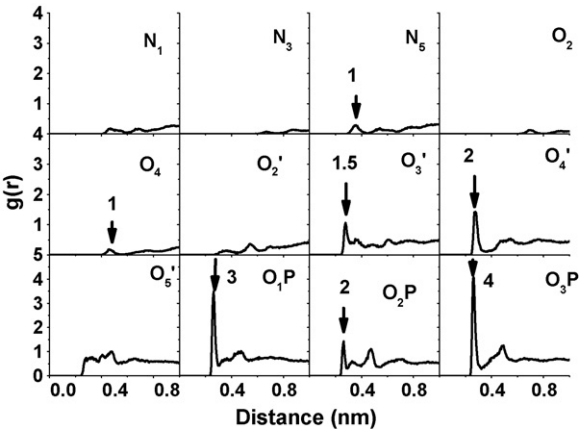

Fig. 13. Radial distribution function of water molecules around FMN in AppA. The radial distribution function, g(r), suggested the presence of two water molecules near O4 and N5 of Iso and ca. 1.5 near O3′, 2 near O4′, 3 near O1P, 2 near O2P, and 4 near O3P in solution. For atom notations, see Fig. 2.

polarity around Iso, Trp104 and Tyr21. There are two anionic groups, Asp24 and Asp70, and one cationic group Arg72 near Iso within 1 nm in AppA, while only one anionic group, Glu13 near Trp32 and Tyr35 within 1 nm in FBP. High polarity in AppA compared to FBP may be ascribed to the presence of these water molecules and ionic groups around ET donors and acceptor.

4. Discussion

Fluorescence decay functions of AppA have been analyzed with KM theory and atomic coordinates obtained by MD. Calculated decays almost exactly duplicated the observed decays. Obtained ET parameters were compared to those of the non-photosensing flavoprotein, FBP (Method 2 in Table 1). ET rate was predicted to be a little faster from Trp104 than from Tyr21 to Iso*. It is striking, however, that the frequency factor ν_0 of Tyr21 was very high ($3226\,ps^{-1}$) in AppA compared to one in FBP ($197\,ps^{-1}$) (Method 2 in Table 1). The frequency factor is related to electronic interaction energy between a donor and an acceptor at the definite donor–acceptor distance. Consequently, ET rate from Tyr21 to Iso* was very fast compared to the expected ET rate (see Fig. S3). ν_0 relates to electronic interaction energy between a donor and an acceptor. Comparing local structures at the Iso binding site between AppA and FBP, Iso in AppA forms H bond chain with Tyr21 through Gln63, while Iso in FBP has no H bond with ET donors. Electronic interaction energy obtained by PM3 method was −11.7 (kcal/mol) in Iso*-Gln63-Trp104. The interaction energy between Iso* and Trp32 was around −24 (kcal/mol) in FBP [53]. In the both systems CT occurred as judged from total charge at Iso*. When the interaction energy is higher, ET rate is faster in FBP [52]. It is not clear why ET from Tyr21 to Iso* was very fast, despite that the interaction energy between Iso* and Tyr21 was little. Two reasons may be conceivable. First, accuracy of the semi-empirical PM3 method may not be good enough for the interaction energy in H bond system, and second, H bond chain from Tyr21 to Iso* might contribute to the fast ET from Tyr21 to Iso*.

Domratcheva et al. [19] have demonstrated by means of MO study with highest level (QM/MM with CASSCF) that almost complete charge transfer takes place from Tyr21 to Iso* (−0.96 at Iso* and +0.93 at Tyr) in the Iso*-Gln63-Tyr21 system. This result supports our finding of very high frequency factor ν_0 of Tyr21 in AppA.

Fast fluorescence quenching in an aromatic H bond system was already reported early in 1956 by Mataga et al. [62]. Subsequently, it was demonstrated that the fast quenching of fluorescence in the H bond π-electronic systems was ascribed to ET through H bond

[63–65], by means of a picosecond-resolved transient absorption spectroscopy. ET from Iso* to Tyr21 may be related to these experimental results.

5. Concluding remarks

ET from Tyr21 is very important for the formation of signaling state of BLUF [12–15] because Y21F AppA displayed inhibition of the photocycle [7,8]. The importance of H bond chain for photosensing function of AppA and other flavin photoreceptors have been pointed out in many earlier works [7–26]. The fast ET from Tyr21 to Iso* was ascribed to extraordinary high frequency factor ν_0 (Tyr21) in KM theory. The high frequency factor may be explained by H bond chain from Tyr21 to Iso* through Gln63. This was supported theoretically [19] as well as experimentally [62–65]. Without the H bond chain ET could be negligible from Tyr21 and mostly take place from Trp104, where signaling state is never formed. Thus the H bond chain in Iso*-Gln63-Tyr21 is essential for enhancement of ET rate, and accordingly for photosensing function of BLUE in AppA.

Acknowledgement

This work was supported by the annual government statement of expenditure of Mahasarakham University (fiscal year 2010). We would like to acknowledge the Computational Chemistry Unit Cell, Chulalongkorn University, for use of the computing facilities.

Appendix A. Supplementary data

Supplementary data associated with this article can be found, in the online version, at doi:10.1016/j.jphotochem.2009.07.020.

References

[1] S. Grosson, K. Moffat, Proc. Natl. Acad. Sci. U.S.A. 98 (2001) 2995–3000.
[2] B. Giovani, M. Brydin, M. Ahmad, K. Brettel, Nat. Struct. Biol. 10 (2003) 489–490.
[3] A. Zeugner, M. Byrdin, J.-P. Bouly, N. Bakrim, B. Giovani, K. Brettel, M. Ahmad, J. Biol. Chem. 280 (2005) 19437–19440.
[4] P.J. Bouly, E. Schleicher, M. Dionisio-Sese, F. Vandenbussche, D. van der Straeten, N. Bakrim, S. Meier, A. Batschauer, P. Galland, R. Bittl, M. Ahmad, J. Biol. Chem. 282 (2007) 9383–9391.
[5] S.-H. Song, N. Öztürk, T.R. Denaro, N.Ö. Arat, Y.-T. Kao, H. Zhu, D. Zhong, S.M. Reppert, A. Sancar, J. Biol. Chem. 282 (2007) 17608–17612.
[6] S. Masuda, C.E. Bauer, Cell 110 (2002) 613–623.
[7] B.J. Kraft, S. Masuda, J. Kikuchi, V. Dragnea, G. Tollin, J.M. Zaleski, C.E. Bauer, Biochemistry 42 (2003) 6726–6734.
[8] W. Laan, M.A. van der Horst, I.H.M. van Stokkun, K. Hellingwerf, J. Photochem. Photobiol. 78 (2003) 290–297.
[9] S. Anderson, V. Dragnea, S. Masuda, J. Ybe, K. Moffat, C. Bauer, Biochemistry 44 (2005) 7998–8005.
[10] S. Masuda, K. Hasegawa, T. Ono, Biochemistry 44 (2005) 1215–1224.
[11] M. Gauden, S. Yeremenko, W. Laan, I.H.M. van Stokkun, J.A. Ihalainen, R. van Grondelle, K.J. Hellingwerf, J.T.M. Kennis, Biochemistry 44 (2005) 3653–3662.
[12] V. Dragnea, M. Waegele, S. Balascuta, C. Bauer, B. Dragnea, Biochemistry 44 (2005) 15978–15985.
[13] W. Laan, M. Gauden, S. Yeremenko, R. van Grondelle, J.T.M. Kennis, K.J. Hellingwerf, Biochem. 45 (2006) 51–60.
[14] M. Gauden, J.S. Grinstead, W. Laan, I.H.M. van Stokkum, M. Avila-Perez, K.C. Toh, R. Boelens, R. Kaptein, R. van Grondelle, K.J. Hellingwerf, J.T.M. Kennis, Biochemistry 46 (2007) 7405–7415.
[15] A. Zirak, A. Penzkofer, T. Schiereis, P.A.J. Hegemann, I. Schlichting, Chem. Phys. 315 (2005) 142–154.
[16] M. Gauden, I.H.M. van Stokkun, J.M. Key, D.C. Lührs, R. van Grondelle, P. Hegemann, J.T.M. Kennis, Proc. Natl. Acad. Sci. U.S.A. 103 (2006) 10895–10900.
[17] A. Jung, J. Reinstein, T. Domratcheva, R.L. Shoeman, I. Schlichting, J. Mol. Biol. 362 (2006) 717–732.
[18] K.C. Toh, I.H.M. van Stokkum, J. Hendrics, M.T.A. Alexandre, J.C. Arents, Biophys. J. 95 (2008) 312–321.
[19] T. Domratcheva, B.L. Grigorenko, I. Schlichting, A.V. Memukhin, Biophys. J. 94 (2008) 3872–3879.
[20] S. Masuda, K. Hasegawa, T. Ono, Biochemistry 43 (2004) 5304–5313.
[21] H. Yuan, S. Anderson, S. Masuda, Y. Dragnea, K. Moffat, C.E. Bauer, Biochemistry 45 (2006) 12687–12694.
[22] R. Takahashi, K. Okajima, H. Suzuki, H. Nakamura, M. Ikeuchi, T. Noguchi, Biochemistry 46 (2007) 6459–6467.
[23] C. Bonetti, T. Mathes, I.H.M. van Stokkun, K.M. Mullen, M.-L. Groot, R. van Grondelle, P. Hegemann, J.T.M. Kennis, Biophys. J. 95 (2008) 4790–4802.
[24] Q. Wu, W.-H. Ko, K.H. Gardner, Biochemistry 47 (2009) 10271–10280.
[25] H. Nagai, Y. Fukushima, K. Okajima, M. Ikeuchi, H. Mino, Biochemistry 47 (2009) 12574–12582.
[26] Y. Fukushima, Y. Murai, K. Okajima, M. Ikeuchi, S. Itoh, Biochemistry 47 (2009) 660–669.
[27] N. Mataga, H. Chosrowjan, Y. Shibata, F. Tanaka, J. Phys. Chem. B (Letter) 102 (1998) 7081–7084.
[28] N. Mataga, H. Chosrowjan, Y. Shibata, F. Tanaka, Y. Nishina, K. Shiga, J. Phys. Chem. B 104 (2000) 10667–10677.
[29] N. Mataga, H. Chosrowjan, S. Taniguchi, F. Tanaka, N. Kido, M. Kitamura, J. Phys. Chem. B (Letter) 106 (2002) 8917–8920.
[30] F. Tanaka, N. Mataga, Trends Chem. Phys. 11 (2004) 59–74.
[31] F. Tanaka, H. Chosrowjan, S. Taniguchi, N. Mataga, K. Sato, Y. Nishina, K. Shiga, J. Phys. Chem. B 111 (2007) 5694–5699.
[32] F. Tanaka, R. Rujkorakarn, H. Chosrowjan, S. Taniguchi, N. Mataga, Chem. Phys. 348 (2007) 237–241.
[33] H. Chosrowjan, S. Taniguchi, N. Mataga, F. Tanaka, D. Todoroki, M. Kitamura, J. Phys. Chem. B (Letter) 111 (2007) 8695–8697.
[34] H. Chosrowjan, S. Taniguchi, N. Mataga, F. Tanaka, D. Todoroki, M. Kitamura, Chem. Phys. Lett. 462 (2008) 121–124.
[35] A. Karen, N. Ikeda, N. Mataga, F. Tanaka, Photochem. Photobiol. 37 (1983) 495–502.
[36] A. Karen, M.T. Sawada, F. Tanaka, N. Mataga, Photochem. Photobiol. 45 (1987) 49–54.
[37] D. Zhong, A. Zewail, Proc. Natl. Acad. Sci. U.S.A. 98 (2001) 11867–11872.
[38] J. Pan, M. Byrdin, C. Aubert, A.P.M. Eker, K. Brettel, M.H. Vos, J. Phys. Chem. B 108 (2004) 10160–10167.
[39] M. Kitamura, S. Kojima, K. Ogasawara, T. Nakaya, T. Sagara, M. Niki, K. Miura, H. Akutsu, I. Kumagai, J. Biol. Chem. 269 (1994) 5566–5573.
[40] K. Suto, K. Kawagoe, N. Shibata, K. Morimoto, Y. Higuchi, M. Kitamura, T. Nakaya, N. Yasuoka, Acta Crystallogr. Sect. D56 (2000) 368–371.
[41] L. Liepinsh, M. Kitamura, T. Murakami, T. Nakaya, G. Otting, Nat. Struct. Biol. 4 (1997) 975–979.
[42] R. Marcus, J. Chem. Phys. 24 (1956) 979–989.
[43] R. Marcus, N. Sutin, Biochim. Biophys. Acta 811 (1985) 265–322.
[44] C. Moser, J. Keske, K. Warncke, R. Farid, P. Dutton, Nature 355 (1992) 796–802.
[45] M. Bixon, J. Jortner, J. Phys. Chem. 95 (1991) 1941–1944.
[46] M. Bixon, J. Jortner, J. Phys. Chem. 97 (1993) 13061–13066.
[47] M. Bixon, J. Jortner, J. Cortes, H. Heitele, M.E. Michel-Beyerle, J. Phys. Chem. 98 (1994) 7289–7299.
[48] T. Kakitani, N. Mataga, J. Phys. Chem. 89 (1985) 8–10.
[49] T. Kakitani, A. Yoshimori, N. Mataga, J. Phys. Chem. 96 (1992) 5385–5392.
[50] T. Kakitani, N. Matsuda, A. Yoshimori, N. Mataga, Prog. React. Kinet. 20 (1995) 347–381.
[51] N. Nunthaboot, F. Tanaka, S. Kokpul, H. Chosrowjan, S. Taniguchi, N. Mataga, J. Photochem. Photobiol. A: Chem. 201 (2009) 191–196.
[52] N. Nunthaboot, F. Tanaka, S. Kokpul, H. Chosrowjan, S. Taniguchi, N. Mataga, J. Phys. Chem. B 112 (2008) 13121–13127.
[53] N. Nunthaboot, F. Tanaka, S. Kokpol, H. Chosrowjan, S. Taniguchi, N. Mataga, J. Phys. Chem. B 112 (2008) 15837–15843.
[54] D. Case, T. Darden, T. Cheatham, C. Simmerling, J. Wang, R. Duke, R. Luo, K. Merz, B. Wang, D. Pearlman, M. Crowley, S. Brozell, V. Tsui, H. Gohlke, J. Mongan, V. Hornak, G. Cui, P. Beroza, C. Schafmeister, J. Caldwell, W. Ross, P. Kollman, AMBER, ver. 8, University of California, San Francisco, 2004.
[55] J.M. Wang, P. Cieplak, P.A. Kollman, J. Comput. Chem. 21 (2000) 1049–1074.
[56] C. Schneider, J. Suhnel, Biopolymers 50 (1999) 287–302.
[57] U. Essmann, L. Perera, M.L. Berkowitz, T. Darden, H. Lee, G. Pedersen, J. Chem. Phys. 103 (1995) 8577–8593.
[58] J.-P. Ryckaert, G. Cicotti, H.J.C. Berendsen, J. Comput. Phys. 23 (1977) 327–341.
[59] V. Vorsa, T. Kono, K.F. Willey, L. Winograd, J. Phys. Chem. B 103 (1999) 7889–7895.
[60] E.R. Henry, R.M. Hochstrasser, Proc. Natl. Acad. Sci. U.S.A. 84 (1987) 6142–6146.
[61] K. Obanayama, H. Kobayashi, K. Fukushima, M. Sakurai, Photochem. Photobiol. 84 (2008) 1003–1010.
[62] N. Mataga, Y. Kaifu, M. Koizumi, Naturwissenshaften 44 (1956) 304–310.
[63] N. Mataga, F. Tanaka, M. Kato, Acta Phys. Polon. 34 (1968) 733–737.
[64] N. Ikeda, H. Miyasaka, T. Okada, N. Mataga, J. Am. Chem. Soc. 105 (1983) 5206–5212.
[65] H. Miyasaka, A. Tabata, S. Ojima, N. Ikeda, N. Mataga, J. Phys. Chem. 97 (1993) 8222–8227.